Intrinsic biochemical noise in crowded intracellular conditions

R. Grima

Citation: J. Chem. Phys. **132**, 185102 (2010); doi: 10.1063/1.3427244
View online: http://dx.doi.org/10.1063/1.3427244
View Table of Contents: http://jcp.aip.org/resource/1/JCPSA6/v132/i18
Published by the American Institute of Physics.

Intrinsic biochemical noise in crowded intracellular conditions

R. Grima[a)]
School of Biological Sciences and Centre for Systems Biology, University of Edinburgh, Edinburgh EH9 3JR, United Kingdom

(Received 10 February 2010; accepted 16 April 2010; published online 14 May 2010)

Biochemical reactions inside cells occur in conditions which are very different than those found *in vitro*. Two of the main characteristic features are the inherently stochastic nature of the reactions and the complex nondilute spatial environment in which they occur. In particular, it is known that the cell interior is crowded by a diverse range of macromolecules which though not participating in a given reaction they will necessarily influence the kinetics through the excluded volume effect and reduction of diffusion coefficients. Current approaches either totally ignore both characteristics of intracellular reactions or else they solely take into account the noisiness via the use of chemical master equations. The latter are valid for a well-stirred gas-phase chemical system and hence are not generally suited to probe kinetics in crowded conditions. We postulate a novel modification of the chemical master equation which enables us to calculate the effects of low to intermediate crowding on the magnitude of the intrinsic noise of intracellular biochemical reactions. The approach is validated for a reversible dimerization reaction in a simple model of a crowded membrane by means of Brownian dynamics. For the typical parameter values characteristic of crowding inside cells, we find that the lack of available volume induces a reduction in the noise intensity of the end products of the reaction and a simultaneous increase in the temporal correlations. This suggests that cells may exert some degree of control on the level of noise in biochemical networks via a purely physical nonspecific effect and that crowding is a source of intracellular colored noise. © *2010 American Institute of Physics*. [doi:10.1063/1.3427244]

I. INTRODUCTION

It is well appreciated that the interior of living cells is not a dilute solution.[1–3] Aqueous solutions are typically characterized by total macromolecular concentrations in the range of 1–10 g/l. In contrast, intracellular concentrations of total protein and RNA in bacterial cells are in the range of 300–400 g/l highlighting the fact that the cytoplasm is more akin to a gel than an aqueous medium. The fraction of the intracellular volume occupied by these macromolecules is estimated to typically lie in the range of 0.20–0.30 for both the cytoplasm[2] and the plasma membrane[4] though values as high as 0.40 have been reported for the cytoplasm of *E. Coli* cells.[5] This condition, popularly known as macromolecular crowding or molecular crowding or simply the excluded volume effect specifically refers to a purely physical nonspecific effect due to steric repulsion.[2] The bulk of these macromolecules do not participate in a given macromolecular reaction but nevertheless exert an influence on its kinetics by decreasing the amount of space available to the center of mass of the reactant molecules. Such molecules are frequently referred to as "crowders" or "crowding agents." Typically the solvent has been considered as a structureless continuum, in which case only solute macromolecules qualify as crowding agents (for a detailed discussion, see Refs. 6 and 7). The free energy is minimized by an increase in the available volume and consequently crowding tends to enhance binding since the latter event generally leads to more compact conformations than those of the reactant molecules. Simultaneously, it is a fact that the macromolecules will serve as inert obstacles for the diffusive encounter of reactant molecules thereby reducing the association rate. It follows that the effect of crowding on reaction kinetics is complex but certainly a significant one as has been already demonstrated by several experiments (for a recent review of the experimental literature, see Ref. 8).

A different but equally important aspect of reactions inside cells is that many molecular species are found to have a low copy number per cell, typically varying from a few tens to few thousands (for an introductory review, see Ref. 9; for a detailed experimental protein abundance study, see, for example, Ref. 10). In general, it is known that the fluctuations in a collection of N particles are roughly of order $N^{1/2}$[11] and hence it follows that intracellular reactions may suffer from considerable intrinsic noise.

The most common method of describing intracellular reaction kinetics, i.e., using sets of coupled ordinary differential equations for the chemical concentrations, ignores both the nondilute nature of the intracellular environment and also the inherent noise. A more faithful approach is provided by the use of chemical master equations (CME), which takes into account the stochastic nature of biochemical reactions but retains the assumption that the system is in a dilute, well-mixed and thermally equilibrated gas-phase (for a recent review, see Ref. 12). Using such a formalism, it is possible to calculate statistical properties of reaction kinetics in small well-mixed compartments (see, for example, Refs. 13–17).

In this article we postulate a novel form of the CME

[a)]Electronic mail: ramon.grima@ed.ac.uk.

which takes into account both the effects of crowding and noise on the kinetics. Within this framework we quantify for the first time the effect of macromolecular crowding on the statistical properties of the intrinsic noise. The theory is subsequently validated using extensive Brownian dynamics simulations of a dimerization reaction in a simple model of a crowded membrane.

II. FORMULATION OF THE CME IN MILDLY CROWDED CONDITIONS

The kinetics of reactions are generally determined by two timescales: (i) τ_d, the typical time it takes for two molecules to find each other via diffusion, and (ii) τ_r, the time for two particles to react given they are within reaction-range distance. If $\tau_d/\tau_r \ll 1$ then we have transition-state limited kinetics; in this case the particles will diffuse thoroughly the compartment many times before a successful reaction occurs. Hence one expects the chemical concentrations to be fairly well-mixed throughout the compartment and the CME to be valid.[9] The other limit, $\tau_d/\tau_r \gg 1$, leads to diffusion-controlled kinetics; a given particle will successfully react in its first few encounters with neighboring particles and hence the kinetics is largely influenced by local fluctuations in the concentration. In this case, a global description such as the CME will not be sufficient, rather a spatially extended description becomes indispensable.

In general one expects that any transition-state limited reaction will tend toward the diffusion-limited regime as the concentration of inert crowding agents is progressively increased since this will have the effect of reducing the diffusion coefficient and of increasing τ_d. Consider a reaction which is transition-state limited in the zero crowding case and hence describable by a CME. Let us say that we now perturb the system by adding a small amount of crowding agents of given size to the mixture. Though the diffusion coefficient will become somewhat smaller, one would expect that the kinetics is still overall dominated by the overcoming of the transition-state barrier. This would suggest that a stochastic kinetics description in terms of an effective CME may still be possible though with different propensity functions than a conventional CME.

Without loss of generality, we now develop our arguments in a quantitative manner for the biologically relevant case of a reversible dimerization reaction, $2A \rightleftharpoons B$ occurring in a compartment of size Ω. The major difference between a CME and the corresponding set of ordinary differential equations is that the former is a mesoscopic description while the latter is a macroscopic one. Small system size, i.e., small volumes, implies a small effective number of interacting particles and considerable intrinsic noise. Hence the CME is necessarily a probabilistic equation and is defined in terms of the absolute number of molecules of each species. More specifically, the CME is a partial differential equation for the probability $P(\vec{n},t)$ of being in state $\vec{n}=(n_1,n_2,\ldots,n_i,\ldots)$ at time t, where n_i is the absolute number of molecules of species I.[11,12] Following our hypothesis in the previous paragraph, the effective CME for the dimerization reaction in the presence of small amounts of crowding agents has the same form as the conventional CME for this reaction but with modified propensity functions

$$\frac{dP(n_a,n_b,t)}{dt} = \frac{\alpha k_f}{2\Omega}(E_a^2E_b^{-1}-1)n_a(n_a-1)P(n_a,n_b,t) + \beta k_r(E_a^{-2}E_b-1)n_bP(n_a,n_b,t). \quad (1)$$

Note that the master equation has been written in a compact form using the step operator $E_i^{\pm m}$ defined by its action on a general function $g(n_i)$ as $E_i^{\pm m}g(n_i)=g(n_i\pm m)$. The constants k_f and k_r are the conventional forward and backward rate constants for the dimerization reaction in the absence of any crowding agents. The functions α and β are the propensity function modifiers and they are presumed to vary with the size, shape and concentration of crowding agents and to have the special property of being equal to one in the limit of zero crowding, i.e., when the occupied volume becomes negligibly small. We note that in reality α and β would have to be also functions of the concentrations and typical sizes and conformational shapes of the molecules participating in a reaction however since we are typically dealing with low copy numbers of reactants inside cells we will assume that the occupied volume stems solely from the crowding agents. The effective equilibrium constant of the reaction is $K=K^0\Lambda$ where $\Lambda=\alpha/\beta$ and $K^0=k_f/2k_r$.

We now solve the master equation exactly in the low-copy number limit, i.e., in the limit when the total number of monomers is at most two. This is the minimum copy number required for the reaction to occur. In this limit, the system alternates between two states: state 1 in which we have two particles of type A and no particles of type B with probability P_1 and state 2 in which we have one particle of type B and no particles of type A with probability P_2. Substituting $n_a=0$ and $n_b=1$ in the effective master equation Eq. (1) and making use of the normalization $P_1+P_2=1$ we obtain

$$\frac{dP_2}{dt} = \frac{\alpha k_f}{\Omega}(1-P_2) - \beta k_r P_2. \quad (2)$$

In the steady-state this has the solution $P_2=\lambda/(1+\lambda)$ where $\lambda=2K^0\Lambda/\Omega$ from which it is straightforward to obtain the m^{th} moment of the number of A and B particles: $\langle n_a^m\rangle = 2^m(1-P_2)$ and $\langle n_b^m\rangle = P_2$. Hence the mean number of dimer B is

$$\frac{\langle n_b\rangle}{\langle n_b\rangle_0} = \frac{\Lambda}{1+\langle n_b\rangle_0(\Lambda-1)}, \quad (3)$$

where $\langle n_b\rangle_0$ is the number of dimer in noncrowded conditions or equivalently in the infinite dilution limit, i.e., in the limit $\alpha,\beta\to 1$. It also follows that the absolute and normalized magnitude of intrinsic noise in A is given by the respective expressions

$$\text{noise}_a = \frac{[\langle n_a^2\rangle - \langle n_a\rangle^2]^{1/2}}{\langle n_a\rangle} = \sqrt{\frac{P_2}{1-P_2}}, \quad (4)$$

$$\epsilon_a = \frac{\text{noise}_a}{\text{noise}_a|_{\alpha,\beta\to 1}} = \sqrt{\Lambda}. \tag{5}$$

Note that ϵ_a is the noise magnitude normalized by the value at infinite dilution. Similarly it is easy to show that generally

$$\epsilon_b = \epsilon_a^{-1}. \tag{6}$$

A measure of deviations from Poissonian behavior is obtained by calculating the standard deviation divided by the square root of the mean which can be interpreted as the width of the actual probability distribution divided by the width of a Poissonian distribution with the same mean:

$$W_a = \sqrt{\frac{[\langle n_a^2\rangle - \langle n_a\rangle^2]}{\langle n_a\rangle}} = \sqrt{2}\left(1 + \frac{\Omega}{2K^0\Lambda}\right)^{-1/2}, \tag{7}$$

$$W_b^2 = 1 - \frac{W_a^2}{2}. \tag{8}$$

Note that this measure quantifies deviations from Poissonian behavior only up till the second moment and hence a value of one is a necessary but not sufficient condition to determine whether the distribution is of the Poisson type or not (this measure is equal to the square root of the commonly used Fano factor). One would have to look at higher moments to ascertain such a fact. Previously, we showed that the moments of B are all equal to $\langle n_b\rangle$; this would be consistent with a Poissonian provided that $\langle n_b\rangle$ is very small which occurs in the limit of a small equilibrium constant or equivalently in the limit $W_b \to 1$. In contrast, evaluating the moments of A at $W_a = 1$, one finds $\langle n_a^m\rangle = 2^{m-1}$ which agrees with those of a Poissonian with the same mean only up to the second moment. In summary, it follows that W_b is a true indicator of deviations from Poissonian behavior whereas W_a simply measures the size of fluctuations relative to that of a Poissonian with the same mean.

As a final statistic, we calculate the autocorrelation of fluctuations in the dimer concentration in steady-state conditions. It can be shown that in general for any Markovian system, the first-order approximation to the autocorrelation time is equal to the time scale of exponential decay associated with the fluctuations about the steady-state values. The equivalence between the two timescales is exact if the mean values follow linear evolution equations as in our case.[18] Since $\langle n_b\rangle = P_2$, it follows from Eq. (2) that the fluctuations δ_b about the steady-state dimer concentration obey the equation: $d\delta_b/dt = -(\alpha k_f/\Omega + \beta k_r)\delta_b$. Hence the autocorrelation time τ for dimer noise is

$$\tau = \left(\beta k_r + \frac{\alpha k_f}{\Omega}\right)^{-1}. \tag{9}$$

A. Estimation of the functions α and β

We now turn to the crucial part of our description, namely, the estimation of the α and β functions. We proceed by observing that the ratio $\Lambda = \alpha/\beta$ is equal to the ratio of the apparent equilibrium constant of a reaction in the presence of crowding agents and of that in the dilute limit. Minton and colleagues[1,8] have estimated this ratio using the scaled particle theory (SPT) of hard-particle fluids. The theory is applicable to transition-state limited reactions between hard particles of any convex shape and is thus ideal for our purposes. In brief, for a general reversible reaction in which i distinct macromolecular solute species react to give m-i new species

$$q_1X_1 + \cdots + q_iX_i \rightleftharpoons q_{i+1}X_{i+1} + \cdots + q_mX_m, \tag{10}$$

with stoichiometric coefficients q_i, standard thermodynamics says that the ratio Λ is given by

$$\Lambda = \prod_{j=1}^{i} \exp\left[\frac{q_jF_j}{RT}\right] \Bigg/ \prod_{j=i+1}^{m} \exp\left[\frac{q_jF_j}{RT}\right], \tag{11}$$

where F_j is the free energy of interaction between a molecule of species j and all of the other solute molecules present in solution. In other words F_j is the work done in introducing a "hole" of free space of size equal to that of a particle of species j in the solution mixture. Note that the presence of inert particles in the mixture will necessarily change F_j and hence the ratio Λ. The free energy can now be estimated using an equation of state derived from the SPT of hard-particle fluids (originally postulated by Reiss *et al.*[19] for a rigid sphere gas and subsequently generalized to any convex hard-particle gas by Gibbons[20])

$$F_j = \sum_{k=0}^{d} A_k R_j^k, \tag{12}$$

where R_j is the characteristic size of a molecule of species j (this is the radius for a spherical molecule) and A_k are positively valued functions of the dimension d, the number concentration, size and shape of all macrosolute species in solution.

It is clear that to make further progress in estimating Λ, we need to specify some further details about our dimerization reaction. We choose the simplest scenario which is consistent with biology: (i) the monomers, dimers and crowders are considered to be cylindrical proteins moving in the plane of the plasma membrane. (ii) a dimer has twice the volume of a monomer implying that the dimer radius r_b is equal to $\sqrt{2}r_a$ where r_a is the monomer radius. (iii) the inert crowders are of a single species with radius r_c. Since the proteins can translate freely only in the membrane plane the problem conveniently reduces to the interaction of hard disks in a two-dimensional plane. With these restrictions it can be shown that the expressions for the free energy and for Λ take the form[4]

$$\frac{F_s}{RT} = -\ln(1-\phi) + 2Q\eta_s + (1+Q)Q\eta_s^2, \tag{13}$$

$$\Lambda = (1-\phi)^{-1}\exp[\,2^{3/2}(\sqrt{2}-1)Q\eta_a)], \tag{14}$$

where $Q = \phi/(1-\phi)$, $\phi = \pi r_c^2\rho_c$ is the fractional area of the membrane occupied by inert crowders with number concentration ρ_c, $\eta_s = r_s/r_c$ is the ratio of the sizes of molecules of species s and crowder particles and s is an index which is either a or b referring to monomer and dimer, respectively. Note that Λ diverges as the size of the crowding molecules r_c

becomes very small. This is a flaw of Minton's theory stemming from the fact that the solvent is assumed to be a structureless continuum; a more complicated approach due to Berg[7] shows that no divergence occurs if one explicitly takes into account steric effects due to solvent molecules. Minton's approach provides approximate quantitative predictions provided there is a clear separation of the two relevant spatial scales: the size of solute macromolecules and the size of the solvent molecules.

Hence our formulation is now complete. The mean number of dimer is given by substituting Eq. (14) into Eq. (3), while Eqs. (5)–(8) together with Eq. (14) give the explicit dependence of the magnitude of intrinsic noise and of the non-Poissonian nature of the noise distribution on the size and concentration of crowding agents. For clarity we here reproduce the full expressions for the intrinsic dimer noise (normalized by its infinite dilution value) and the fractional width of the probability distribution of the dimer noise relative to a Poissonian of the same mean

$$\epsilon_b = \sqrt{1-\phi}\,\exp\left[-(2-\sqrt{2})\frac{\phi}{1-\phi}\frac{r_a}{r_c}\right], \tag{15}$$

$$W_b = \left(1+\frac{2K_0}{(1-\phi)\Omega}\exp\left[2^{3/2}(\sqrt{2}-1)\frac{\phi}{1-\phi}\frac{r_a}{r_c}\right]\right)^{-1/2}, \tag{16}$$

$$W_a = \sqrt{2(1-W_b^2)}. \tag{17}$$

Thus it follows that as we increase the extent of crowding, i.e., the number density of crowders and the ratio of the sizes of monomer and crowder particles, the magnitude of intrinsic noise in the dimer diminishes while the probability distribution of the dimer noise becomes increasingly non-Poissonian. From Eqs. (6) and (8), we see that the reverse statement is correct for the statistics of monomer noise. We defer a full discussion of the physics behind these effects and their biological relevance to Sec. IV.

It is interesting to note that the autocorrelation defies explicit evaluation since it is not a function of Λ but rather requires the exact dependence of α and β on the crowding parameters; the latter is not presently known though it has been hypothesized by Minton[21] that this is a strong function of the correlation between the shape of the transition-state complex and the shapes of the reactant and product molecules.

III. BROWNIAN DYNAMICS SIMULATIONS

In Sec. II, we have postulated a modification of the CME by rescaling the propensity functions according to SPT. Using this new formulation, we solved the CME in the low copy number limit since under such conditions it can be solved exactly. We now want to test the validity and accuracy of the derived noise statistics. A simulation method on a finer spatial scale than the CME is thus needed. We choose Brownian dynamics since it is straightforward to implement, particularly for our two monomer system (the system is schematically illustrated in Fig. 1). The algorithm is described in detail in subsection A.

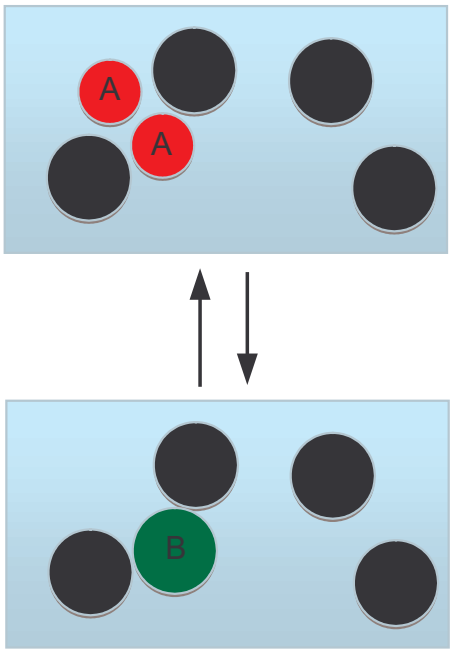

FIG. 1. Schematic illustrating our simplified model of a dimerization reaction in a crowded membrane. The disks represent cylindrical transmembrane proteins as would be "viewed from above." The black disks are the inert crowding proteins. In the low copy number limit, at any one time, the system can only be in two states: state 1 with 2 monomers and 0 dimers (top diagram) and state 2 with 0 monomers and 1 dimer (bottom diagram).

A. Algorithm

1. Initially two monomers, i.e., two disks of radius r_a are placed at the center of a square with side length $\sqrt{\Omega}$ and with separation between their centers equal to $4r_a$. A number of crowder disks of radius r_c are randomly distributed in the square. The zero overlap condition is enforced for all particles at all times.
2. At each time step, a particle is randomly picked. Its two-dimensional diffusion is modeled via a Langevin equation, $dx(t)/dt=\zeta(t)$, where $x(t)$ is the particle's position at time t and ζ is a stochastic random variable with the properties $\langle\zeta(t)\rangle=0$ and $\langle\zeta(t)\zeta(t')\rangle=2D\delta(t-t')$. The diffusion coefficient D is computed according to the radius of the chosen particle using the Saffman–Delbruck equation (see later discussion regarding the use of this equation). A spatial displacement is rejected if this results in an intersection with another particle.
3. If the chosen particle is a monomer and diffusion causes it to intersect with another monomer then we check if a hypothetical new dimer placed at the center of mass coordinates of the two monomers would intersect with any crowder; if there is no intersection the reaction occurs with probability p_f, the monomers are destroyed and the hypothetical dimer becomes a real one.
4. If the particle is a dimer then we check if two hypothetical new monomers which are touching but not intersecting and whose center of mass coordinates coincides with that of the dimer would overlap with any crowders; if no intersection, the reverse reaction occurs with probability p_r resulting in the elimination of the

dimer and replacement by the two new monomers. Note that the angle subtended by the line passing through the center of mass of the hypothetical monomers and the coordinate axes is chosen from a uniform random distribution.

5. Steps 2–4 are iterated a number of time steps equal to the number of distinct particles at the beginning of this loop; the real time is then incremented by one. This procedure ensures that every particle is chosen on average once per unit time step.

Periodic boundary conditions are enforced. As mentioned in step 2 of the above algorithm, the diffusion coefficient of particles is that given by the Saffman–Delbruck equation.[22] This equation gives the diffusion coefficient of an incompressible cylinder in a membrane in terms of the cylinder radius, the membrane thickness and the viscosities of the membrane and adjacent fluid. The cylinder radius exactly coincides with the radius of our disklike molecules. Recent mesoscopic simulations using dissipative particle dynamics have verified that the lateral diffusion coefficient of proteins is well described by the Saffman–Delbruck equation for protein radii less than about 7.4 nm.[23] A single time step in our simulation is set to represent 0.06 μs of real time; this ensures that the maximum spatial displacement due to diffusion is an order of magnitude smaller than the diameter of the smallest protein.

One may note that the initial conditions in step 1 is such that the separation between monomers is fixed to $4r_a$ and wonder why we do not average over different initial conditions. We initially conducted simulations with various initial separations and found that the steady-state mean number of particles and the statistics of intrinsic noise were always independent of the initial conditions, the only visible difference being the time to reach steady-state. Hence we fixed the initial condition so that the monomers are not too far from each other which minimizes the time to steady-state and consequently allows us to garner very good statistics in reasonable computational time.

In essence, our simulation algorithm captures the combined lateral diffusion and reaction of two cylindrical monomer proteins in the presence of a single species of inert cylindrical protein crowders in the plasma membrane. We note that our Brownian dynamics simulation algorithm is similar in spirit to the one by Lee *et al.*[24] but is not implemented using their Green's function reaction dynamics method.

B. Parameter values and method of data extraction

The radius of the crowders was fixed to 2 nm, a typical transmembrane protein size.[4] The probabilities per unit time for the forward and backward reactions, p_f and p_r, were varied over the range of $10^{-3}-10^{-1}$. Equations (15)–(17) suggest that the two major relevant simulation parameters are the occupied area fraction, ϕ and the relative size of monomer to crowder particle, r_a/r_c. Hence we did two types of simulations. In the first type, we studied the effect of increasing occupied area fraction on the noise statistics at constant ratio of the size of monomer and crowder particles while in the second type we studied the effect of increasing the ratio of the size of monomer and crowder particles on the noise statistics at constant area fraction. We now give the details for both types of simulation.

(1) Simulations at constant r_a/r_c with varying ϕ. The radius of the monomer is fixed to 2 nm (i.e., $r_a=r_c$), the membrane patch is fixed to a side length of 40 nm and the total number of crowders is varied so that the occupied area fraction ϕ ranges from 0 to 0.4. The latter is simply calculated as the total cross-sectional area of the crowders divided by the area of the membrane patch.

(2) Simulations at constant ϕ with varying r_a/r_c. The radius of the monomer is varied between 2 and 5 nm in steps of a nanometer. The number of crowders is chosen so that ϕ is fixed to 0.3 (an approximately typical value for real membranes[4]). The side length of the membrane patch is chosen so that the ratio of the side length to monomer radius is equal to 20 in all cases. This reduces finite-size effects and ensures that the area fraction occupied by two monomers is fixed to 0.015708, a value which is much smaller than the area fraction occupied by crowders.

In all cases, we obtained data from a set of 8 long time simulations. The long-time averaging over each one of these simulation data leads to eight independent estimates of the steady-state statistical quantities: $\langle n_a\rangle$, $\langle n_b\rangle$, $\langle n_a^2\rangle$, $\langle n_b^2\rangle$, $\langle n_b(t)n_b(t+T)\rangle$, N_a, and N_d. Note that $\langle n_b(t)n_b(t+T)\rangle$ is the correlator with time lag T, while N_a and N_d are the average number of association and dissociation events per unit time. The quantities ϵ_a, ϵ_b, W_a, and W_b can be computed directly from their basic definitions in terms of the simulation measured moments of the number of monomer and dimer particles at steady-state. The autocorrelation time is obtained by fitting an exponential to the graph of the numerically estimated correlator versus lag time. The functions α and β are computed from N_a and N_d as follows. The number of dissociation events per unit time must be equal to the probability of the system being in the dimer state multiplied by the probability of dissociation per unit time, i.e., $N_d=\langle n_b\rangle\beta p_r$ from which β can be directly computed. Similarly the number of association events per unit time must be proportional to the probability of the system being in the two monomer state multiplied by the probability of association per unit time, i.e., $N_a=c(1-\langle n_b\rangle)\alpha p_f$. Note that c is some fractional constant which takes into account the fact that the effective probability of forward dimerization reaction is in the dilute-limit less than p_f because monomers must be brought in close spatial proximity before a reaction occurs (i.e., c must be inversely proportional to the area of the membrane patch). We estimate this constant for the case of zero crowding agents and then use the above formula to obtain α. For all of the above statistical quantities we have a set of eight long-time averaged values from which we then compute an averaged quantity and the standard deviation about it which is what is shown in the graphs discussed in Sec. IV.

The long-time averaging was conducted over the interval $[10^6, 15\times10^6]$ for simulations of type (1) and over the inter-

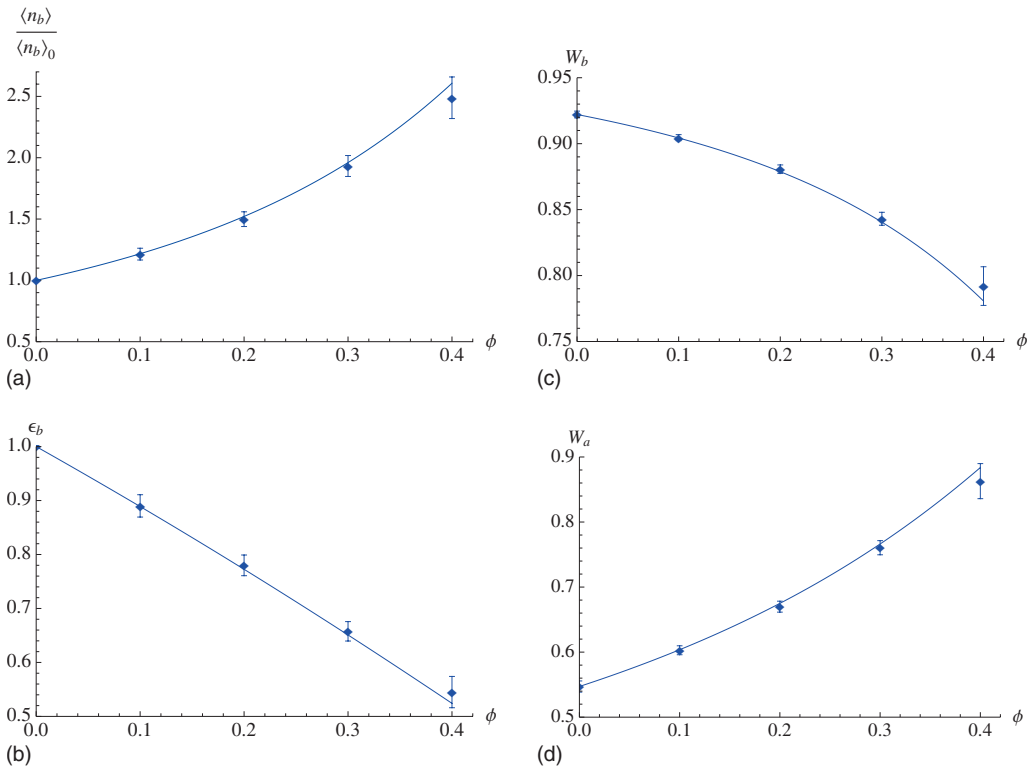

FIG. 2. Dependence of the statistics of intrinsic noise on the occupied area fraction of the membrane. The plots show the variation of (a) the normalized mean number of dimer, (b) the normalized magnitude of intrinsic noise in the dimer concentration, ϵ_b, (c) the non-Poissonian measure, W_b, and (d) the non-Poissonian measure, W_a, with the occupied area fraction of the membrane ϕ due to inert crowders. The monomers and crowders have radius 2 nm and the dimer has a cross-sectional area twice of the monomer. The probability per unit time of association and dissociation are p_f=0.1 and p_r=0.001. In (a) and (b) the normalization is with respect to the value in the absence of any crowders. $W_a(W_b)$ is the width of the probability distribution of intrinsic monomer (dimer) noise divided by the width of a Poisson distribution with the same mean. The data points are obtained from Brownian dynamics simulation. The solid lines show the theoretical results given by (a) Eq. (3) together with Eq. (14), (b) Eq. (15), (c) Eq. (16), and (d) Eq. (17).

val $[10^6, 60\times 10^6]$ for simulations of type (2). Note that time is here reported in terms of the number of unit time steps. Note also that steady-state conditions are guaranteed over the mentioned time intervals since the beginning of the logging time (10^6) is a thousand times larger than the characteristic decay time of the slowest reaction with probability per unit time 10^{-3}.

IV. RESULTS AND DISCUSSION

In this section, we present our simulation results, compare with the theory developed in Sec. II and discuss their broader relevance to the biochemistry and physics of intracellular reactions. The results of the data analysis from simulations exploring the dependence of the statistics of intrinsic noise with varying occupied area fractions ϕ and ratios of the sizes of monomer and crowder particles r_a/r_c are shown in Figs. 2 and 3. Data points are the simulation results while the solid lines is the theory (see figure captions for details). The comparison of the theoretical and simulation values of W_a and W_b requires the evaluation of the constant K_0 in Eqs. (16) and (17); this is chosen by equating the theoretical expressions to the numerical value of W_b and W_a estimated from the simulations at zero crowding. Note also that the size parameter Ω in our equations is the area of the membrane.

Figure 2 shows the simulation results for the case in which monomer and crowding particles are of equal size. The agreement between theory and simulation is very good; indeed this is quite surprising at the higher occupied area fractions since one here expects more significant diffusion-limitation effects. Crowding is found to stabilize the dimer state, decrease the magnitude of intrinsic dimer noise, increase the non-Poissonian nature of the dimer fluctuations, and to "push" the monomer fluctuations toward those expected from a Poisson distribution. All these effects are relative to the case of zero crowding, ϕ=0. These results verify our initial hypothesis that by choosing the renormalized propensity functions constants in an effective CME according to the prescription of SPT we can qualitatively and quantitatively predict the statistics of intrinsic noise in a crowded environment, one which is not necessarily perfectly well-mixed as in the conventional application of the CME.

From a biological point of view, the statistics of the fluctuations in the end products of a reaction are probably the most significant since these will feed into downstream networks. Our results suggest that crowding enhances the probability of being in the dimer state [Fig. 2(a); we will refer to this as stabilization of the dimer state] and acts to diminish the magnitude of the dimer (the end product in our case) fluctuations [Fig. 2(b)]; this occurs because of two main reasons: (i) in the crowded state, a dimer is less likely to decay since putting two monomers side by side instead of a dimer occupies more space than the latter and hence has a higher chance of overlapping with crowders which is not allowed due to steric repulsion. (ii) Even if a decay occurs, the mono-

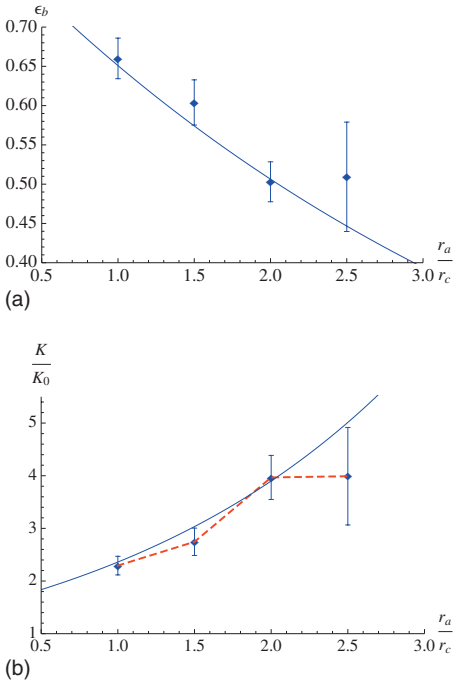

FIG. 3. Dependence of the statistics of intrinsic noise on the ratio of the sizes of monomer and crowder particles. Plots showing the variation of (a) the normalized magnitude of intrinsic noise in the dimer concentration, ϵ_b, (b) the apparent normalized equilibrium constant with the ratio of the sizes of monomer and crowder particles, r_a/r_c, at fixed occupied area fraction of the membrane ϕ equal to 0.3. The normalization is with respect to values in the absence of any crowders. Crowders have a fixed radius of 2 nm, while monomer radius is varied from 2 to 5 nm in steps of 1 nm; in all cases dimer has a cross-sectional area twice of the monomer. The probability per unit time of association and dissociation are p_f=0.01 and p_r=0.001. The data points are obtained from Brownian dynamics simulation. The solid line shows the theoretical results: Eq. (15) for (a) and Eq. (14) for (b). The red dashed line in (b) joins the means and by comparison with the solid line illustrates the breakdown of the transition-limited kinetics assumption [solid line in (b)] at large ratios of the sizes of monomer and crowder particles.

mers will not be able to leave this spatial site so easily as in the dilute case due to a local caging effect by the crowders, which naturally enhance the probability of a successful recollision. In the dilute limit, dimer production events are rare and practically independent of each other (because diffusion between two such successive events occurs for long times and hence erases any memory of the previous dimer formation event) suggesting Poisson statistics for dimer noise; crowding enhances spatiotemporal correlations between successive dimer formation events and thus causes deviations from Poissonian behavior [Fig. 2(c)]. We note that monomer fluctuations are always non-Poissonian because their production or decay always occurs in pairs and thus not independently of one another.[11] The fact that W_a appears to approach one with increasing crowding [Fig. 2(d)] is thus not indicative of the underlying probability distribution becoming Poissonian but rather it shows that monomer fluctuations become harder to suppress with increasing crowding due to a destabilization of the two monomer state.

The results of a similar data analysis but from simulations exploring the dependence of intrinsic noise statistics with varying r_a/r_c at constant ϕ=0.3 is shown in Fig. 3(a). The overall tendency of the magnitude of intrinsic noise to decrease with increasing crowding is found to be valid for all monomer sizes until the apparent critical size, r_a/r_c=2.5. At this point the standard deviation is very large even though the averaging is done over a very long time and the average noise magnitude is considerably different from the theoretical prediction. This can be explained as follows. It has been postulated that the apparent equilibrium constant increases for small amounts of crowding but that for large enough amounts diffusion-limitation causes it to start decreasing (see Fig. 3 of Ref. 1). Since the normalized dimer noise magnitude is generally inversely proportional to the apparent equilibrium constant of the reaction, as shown by Eqs. (5) and (6), it follows that when a certain critical amount of crowding is reached ϵ_b should stop decreasing and start to slowly increase with increasing r_a/r_c. For our case this suggests that kinetics start to become dominated by diffusion-limitation in the region of $r_a/r_c \simeq 2.5$. To test this hypothesis we computed the effective equilibrium constant from our simulation data [Fig. 3(b)]; the solid line is the estimate Λ as given by Eq. (14) which as mentioned earlier is valid in the region where kinetics are transition-state limited. Note that the computed apparent equilibrium constant (red dashed lines) reaches a maximum at r_a/r_c=2.5 which marks the beginning of the diffusion-limited kinetics regime (compare with Fig. 3 of Ref. 1) and which hence further validates the physical reason behind the discrepancy of the theoretical and simulation values of ϵ_b for large ratios of the sizes of monomer and crowder particles.

We now explore how the autocorrelation of noise depends on crowding. The variation of the autocorrelation time of dimer noise with ϕ for the case of equally sized monomer and crowding particles is shown in Fig. 4(a). The autocorrelation time is here normalized by the value for ϕ=0. The monotonic increase in the autocorrelation time of dimer noise mirrors the tendency of the dimer, once it is formed, to stay in that state and to quickly revert back to dimer state if by chance it decays into a two monomer state. In this case, we have no explicit theoretical prediction since Eq. (9) depends on the absolute magnitude of α and β rather than on their ratio Λ. For comparison, we plot as a dashed line the function Λ as given by Eq. (14) and note the apparent similarity between this function and the autocorrelation time. From Eq. (9), it is possible to get $\tau/\tau_0 \simeq \Lambda$ if $\alpha \simeq 1$ (i.e., $\Lambda \simeq 1/\beta$) and $2K^0/\Omega \ll 1$. This would suggest that for the case of monomer equal in size to crowder, crowding affects primarily the dissociation rate (decreases it) and has little effect on the association rate. This is indeed confirmed by computing the functions α and β from simulation [Fig. 4(b)]. These graphs indicate that for monomers equal in size to crowders it is found that (i) the effective association constant increases slightly with the occupied area fraction ϕ up till ϕ=0.3 and then starts to decrease; this is consistent with the classical idea that the association rate is a sum of an enhancement factor due to increased effective concentrations and an attenuation factor due to reduced diffusion encounter rates.[2] (ii) The dissociation constant decreases monotonically with ϕ. In the classical literature of crowding, there is little mention of crowding having an impact on the dissociation rate. However recent theory, experiment and simulation all show that such an effect is a realistic phenomenon.[21,24,25] As

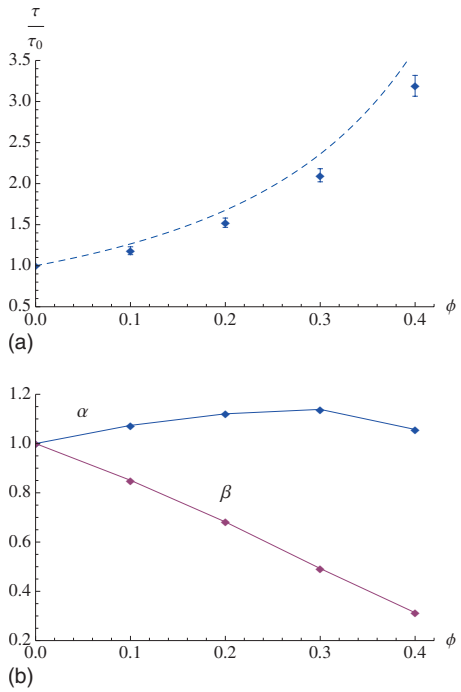

FIG. 4. Dependence of the autocorrelation time of dimer fluctuations and of the propensity function modifiers on the occupied area fraction of the membrane. Plots showing the variation of (a) the normalized autocorrelation time τ/τ_0, (b) the propensity function modifiers, α and β, with the occupied area fraction of the membrane ϕ due to inert crowders. The normalization in (a) is with respect to the value in the absence of crowders. The monomers and crowders have radius 2 nm and the dimer has a cross-sectional area twice of the monomer. The probability per unit time of association and dissociation are $p_f=0.1$ and $p_r=0.001$. In (a) the data points are obtained from Brownian dynamics simulation, while the dashed line shows the function Λ as given by Eq. (14). This illustrates that in this case the autocorrelation time has a similar dependence on the area fraction as the theoretical equilibrium constant of the reaction. In (b) all data is from simulation, the solid connecting lines being simply a guide to the eyes.

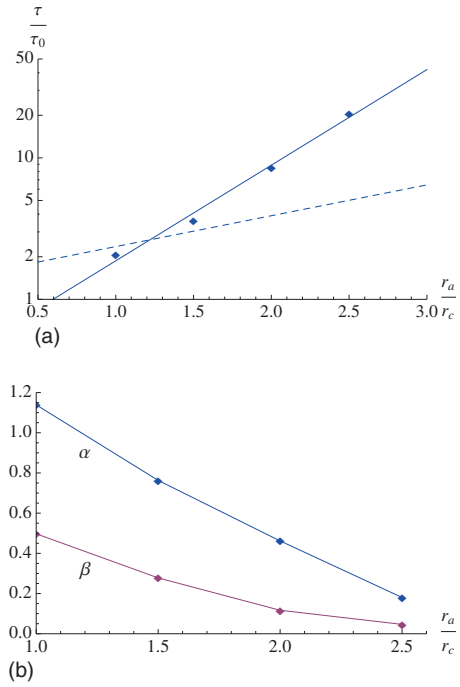

FIG. 5. Dependence of the autocorrelation time of dimer fluctuations and of the propensity function modifiers on the ratio of the sizes of monomer and crowder particles. Plots showing the variation of (a) the normalized autocorrelation time τ/τ_0, (b) the propensity function modifiers, α and β, with the ratio of the sizes of monomer and crowder particles, r_a/r_c. The occupied area fraction of the membrane ϕ due to inert crowders is fixed to 0.3. The normalization in (a) is relative to the autocorrelation in the absence of crowders. Crowders have a fixed radius of 2 nm, monomer radius is varied from 2 to 5 nm in steps of 1 nm; in all cases dimer has a cross-sectional area twice of the monomer. The probability per unit time of association and dissociation are $p_f=0.01$ and $p_r=0.001$. In (a) the data points are obtained from Brownian dynamics simulation, the solid line is a best fit exponential through the data points and the dashed line is the normalized theoretical equilibrium constant of the reaction Λ. Note that the autocorrelation time has generally an exponential dependence on r_a/r_c, which is not the same as Λ except when $r_a=r_c$ (also shown in Fig. 4a). In (b) all data is from simulation, the solid connecting lines being simply a guide to the eyes.

pointed out by Minton[21] whether crowding impacts primarily the association or dissociation rates depends on the conformation of the transition state relative to that of the reactants and products. This may indicate that the autocorrelation time unlike the other measured statistical quantities may depend on the exact details of the method of molecular simulation and thus it maybe difficult to probe with a mesoscopic simulation method.

The dependence of the autocorrelation time of dimer noise with r_a/r_c at constant ϕ is explored in Fig. 5(a). Once again this monotonically increases with crowding due to a stabilization of the dimer state. The solid line is the best exponential fit through the data points while the dashed line is the function Λ. Note that the two approximately agree only for $r_a \simeq r_c$ [as also shown in Fig. 4(a)] but otherwise are different. Some insight is possible by noting that Eq. (9) reduces to $\tau/\tau_0 \simeq \Lambda/\alpha$ in the limit of very small K^0/Ω. This suggests that as the monomer size increases beyond that of the crowder, the association constant starts to rapidly decrease (in contrast this was approximately constant for the previous case in which monomer and crowder had equal size). This also agrees with a numerical estimation of α and β from simulation [Fig. 5(b)]. The decrease of the rate of association can be readily explained by increasing diffusion-limitation effects. We note that our results are consistent with those reported by Lee *et al.*[24] whose data indicated that the dissociation constant decreased relative to the association constant with increased crowding. Our results show that when this is the case, the autocorrelation time will invariably increase with the extent of crowding and since the autocorrelation time of noise determines its color, it follows that there exists the distinct possibility that crowding enhances the color of intrinsic noise inside cells. This strongly correlated noise will naturally feed into other downstream biochemical networks and modulate their input-output characteristics.

We note that although the results shown in the graphs are specifically for probabilities of association and dissociation per unit time equal to $p_f=0.1, p_r=0.001$ or $p_f=0.01, p_r=0.001$, we have found that all the above results hold true in the explored range $p_f, p_r=\{10^{-3}-10^{-1}\}$. This can be appreciated by noting the very good agreement between the values of ϵ_b at $r_a/r_c=1$ and $\phi=0.3$ from Figs. 2(b) and 3(a); similar excellent agreement is found for the autocorrelation time by a comparison of Figs. 4(a) and 5(a).

In this article we have postulated a new form of the

nonspatial chemical master equation which describes the stochastic kinetics of reactions in a crowded medium such as the intracellular environment. By renormalizing the propensity functions according to the SPT of hard-particle fluids, we show that the resultant CME explicitly predicts how the statistics of intrinsic noise are modified in a crowded environment compared to those in a dilute one. These predictions are carefully checked by comparison with off-lattice Brownian dynamics simulations of a dimerization reaction in a membrane. The mesoscopic theory fares remarkably well for occupied area fractions and particle sizes characteristic of macromolecular crowding. The breakdown of the theory inevitably occurs when the kinetics become strongly dominated by diffusion in which case an explicit spatial description becomes naturally indispensable. Previous studies have shown that noise can be attenuated by certain elements of a reaction pathway, for example, negative feedback;[13] here we demonstrate that such attenuation is also effectively brought about by constraining the reaction to occur in a crowded region of the intracellular environment. Cellular control of the local crowdedness would enable simultaneous modulation of the rates of a reaction and of the intrinsic noise, a desirable quality. Although we have proved this specifically for the case of a dimerization reaction, the same attenuation mechanism is generally true for any reaction provided its apparent equilibrium constant increases in the presence of crowding agents; this is the case if the end products of a reaction exclude less volume to crowder than the reactants. We have also shown that crowding can in some instances significantly increase the autocorrelation of noise in the end products implying that it is a potential source of colored noise inside cells. This noise feeds into downstream networks and due to its inherently long correlation timescales it will significantly impact their function and performance.[26] Concluding, we have developed a novel effective chemical master equation which describes the combined influence of intrinsic noise and crowding on stochastic chemical kinetics inside cells. Future work will concentrate on applying the formalism to more general reaction pathways in a three-dimensional space with distributions of inert crowding particles of various shapes and sizes.

ACKNOWLEDGMENTS

We thank Allen P. Minton and Christian Fleck for useful discussions. Support from SULSA (Scottish Universities Life Sciences Alliance) is gratefully acknowledged.

[1] S. B. Zimmerman and A. P. Minton, Annu. Rev. Biophys. Biomol. Struct. **22**, 27 (1993).
[2] R. J. Ellis, Curr. Opin. Struct. Biol. **11**, 114 (2001).
[3] O. Medalia, I. Weber, A. S. Frangakis, D. Nicastro, G. Gerisch, and W. Baumeister, Science **298**, 1209 (2002).
[4] B. Grasberger, A. P. Minton, C. DeLisi, and H. Metzger, Proc. Natl. Acad. Sci. U.S.A. **83**, 6258 (1986).
[5] S. B. Zimmerman and S. O. Trach, J. Mol. Biol. **222**, 599 (1991).
[6] D. Hall and A. P. Minton, Biochim. Biophys. Acta **1649**, 127 (2003).
[7] O. G. Berg, Biopolymers **30**, 1027 (1990).
[8] H. X. Zhou, G. Rivas, and A. P. Minton, Annu. Rev. Biophys. **37**, 375 (2008).
[9] R. Grima and S. Schnell, Essays Biochem. **45**, 41 (2008).
[10] Y. Ishihama, T. Schmidt, J. Rappsilber, M. Mann, F. U. Hartl, M. J. Kerner, and D. Frishman, BMC Genomics **9**, 102 (2008).
[11] N. G. VanKampen, *Stochastic Processes in Physics and Chemistry* (Elsevier, New York, 2007).
[12] D. T. Gillespie, Annu. Rev. Phys. Chem. **58**, 35 (2007).
[13] M. Thattai and A. van Oudenaarden, Proc. Natl. Acad. Sci. U.S.A. **98**, 8614 (2001).
[14] D. Gonze, J. Halloy, and A. Goldbeter, Proc. Natl. Acad. Sci. U.S.A. **99**, 673 (2002).
[15] J. M. G. Vilar, H. Y. Kueh, N. Barkai, and S. Leibler, Proc. Natl. Acad. Sci. U.S.A. **99**, 5988 (2002).
[16] R. Grima, Phys. Rev. Lett. **102**, 218103 (2009).
[17] R. Grima, BMC Syst. Biol. **3**, 101 (2009).
[18] C. W. Gardiner, *Handbook of Stochastic Methods for Physics, Chemistry and the Natural Sciences* (Springer, New York, 2004).
[19] H. Reiss, H. L. Frisch, and J. L. Lebowitz, J. Chem. Phys. **31**, 369 (1959).
[20] R. M. Gibbons, Mol. Phys. **17**, 81 (1969).
[21] A. P. Minton, Biophys. J. **80**, 1641 (2001).
[22] P. G. Saffman and M. Delbruck, Proc. Natl. Acad. Sci. U.S.A. **72**, 3111 (1975).
[23] G. Guigas and M. Weiss, Biophys. J. **91**, 2393 (2006).
[24] B. Lee, P. R. LeDuc, and R. Schwartz, Phys. Rev. E **78**, 031911 (2008).
[25] J. M. Rohwer, P. W. Postma, B. N. Kholodenko, and H. V. Westerhoff, Proc. Natl. Acad. Sci. U.S.A. **95**, 10547 (1998).
[26] V. Shahrezaei, J. F. Ollivier, and P. S. Swain, Mol. Syst. Biol. **4**, 196 (2008).